Primitive chain Brownian simulations of entangled rubbers

Short title: Simulations of entangled rubbers

J. Oberdisse[1,2], G. Ianniruberto[2], F. Greco[3], G. Marrucci[2]

[1] Laboratoire Léon Brillouin CEA/CNRS
CEA Saclay F-91191 Gif sur Yvette, France
[2] Dipartimento di Ingegneria Chimica
Università degli studi di Napoli "Federico II"
Piazzale Tecchio 80, I –80125 Napoli, Italy
[3] Istituto per la Tecnologia dei Materiali Compositi - CNR
Piazzale Tecchio 80, I –80125 Napoli, Italy

PACS 61.41.+e Polymers, elastomers, and plastics
83.20.Jp Computer simulation

Abstract

We present a new multi-chain Brownian dynamics simulation of a polymeric network containing both crosslinks and sliplinks (entanglements). We coarse-grain at the level of chain segments connecting consecutive nodes (cross- or slip-links). Affine displacement of nodes is not imposed; rather, their displacement as well as sliding of monomers through sliplinks is governed by force balances. The stress-strain response in uniaxial extension is compared with the sliplink theories of Ball et al. [*Polymer*, **22** (1981) 1010] and Edwards and Vilgis [*Polymer*, **27** (1986) 483], and with the molecular dynamics simulations of Grest et al. [*J. Non-Cryst. Solids*, **274** (2000) 139]. Qualitative agreement both with the Mooney-Rivlin expression and with the stress upturn at large strains confirms the role of entanglements in explaining departure from the classical theory of phantom chain networks. However, quantitative agreement with data is satisfactory at low strains only, and the observed discrepancy at larger strains suggests possible refinements of the model. Additivity of free energy contributions of crosslinks and entanglements used in several molecular theories of rubber elasticity is confirmed by the simulation results.

Introduction

Rubber elasticity has been a topic of interest for over half a century [1]. Experimentally, stress-strain isotherms are rather easy to measure, but the elimination of network imperfections like dangling ends and spatial heterogeneities still is a major challenge [2]. From a theoretical point of view, the original affine and phantom network theories [3] have been modified to account for entanglements. In one approach the assumption is made that entanglements constrain fluctuations of the network chains only at the junctions [4], a concept later extended to include constraints acting also along the chain contour [5]. In another approach the topological constraint is treated directly as a mean field acting all along the chain, i.e., through a tube model [6, 7]. All such theories are essentially single-body theories of entanglements; many-chain approaches were followed – to our knowledge – only in two cases. One is the network model with cross- and slip-links by Ball *et al*. [8], which makes use of the 'replica' formalism of statistical mechanics, also employed by Panyukov [9]. The model of Ball *et al*. [8] was later extended by Edwards and Vilgis [10] to account for the finite extensibility of the chains. The second many-chain approach is the molecular dynamics simulation of bead-spring chains developed in the past decade by Kremer and coworkers [11-13]. The latter authors made no special assumption on the topological interaction, which is automatically enforced through excluded volume effects. Their simulations have produced a number of interesting results, ranging from the detailed statistics of subchains between entanglements up to the macroscopic mechanical response to deformation. All these results, however, are computationally expensive, and supercomputers must be used.

In this letter we present a new many-chain Brownian dynamics simulation of entangled networks, where chains are modeled on a *coarser* scale than in the simulations mentioned above. Indeed, our model is constructed in close analogy to the primitive chain concept [6, 14], with sliplinks representing binary topological interactions as in Ball *et al*. [8]. This allows a considerable gain in computing time as compared to the work of Kremer and coworkers [11-13], although local features (below the size of subchains between entanglements) are obviously lost. It is hoped, however, that significant predictions on the macroscopic rheological properties can still be achieved.

The results reported in this letter refer to a monodisperse end-linked rubber, with up to ca. 20 entanglements per chain. However, other situations can readily be examined, and an extension of the method to melts has already been proposed [15].

Description of the simulation

We briefly outline the framework of our simulation, leaving further details to a future publication. The first step in the network construction consists in creating a number of bead-spring chains of fixed steplength in a 3D cubic box, with periodic boundary conditions. The end beads of the chains are then used to form crosslinks, whereas each internal bead is connected to one (and only one) other internal bead through a sliplink, which simulates an entanglement. Indeed, a recent molecular dynamics simulation of melts identified entanglements as long-lived *binary* contacts between chains [16].

The network is built up from the chains by connection of beads that are spatially close, where "closeness" is defined through an appropriate search radius. The linking conditions are as follows: (i) crosslinks must have a functionality f not larger than 4 ; (ii) internal beads only connect themselves in pairs (f = 4), and the two partner beads must not be nearest neighbours along the same chain; (iii) the resulting network is accepted only if defects are but a few, i.e., if its average functionality falls in the interval $3.9 < f < 4$.

Once the network has been formed, it is equilibrated by switching on the dynamics (see below). The statistical properties of the network can be tuned by carefully choosing the network parameters (initial steplength, subchain density, etc.) so that the equilibrated network is made to obey Gaussian statistics down to the subchain level, as indeed experimentally observed in undeformed dry networks [17]. For each subchain, we use the Gaussian force law

$$\mathbf{F} = \frac{3kT}{nb^2}\mathbf{a} \tag{1}$$

where b is the Kuhn segment (or "monomer") length, and n and **a** are monomer number and end-to-end vector of the subchain, respectively.

Alternatively, in order to account for finite chain extensibility, we will use a simple non-Gaussian modification consisting in multiplying the force in eq. (1) by the scalar factor $1/(1-a^2/n^2b^2)$ [18].

Brownian dynamics of our network with entanglements is simulated by two types of motion. One of them is node motion (slip- and cross-links alike), due both to thermal agitation and to the net force resulting from the subchains pulling on the node. For the Gaussian case, the discretised equation of node motion reads (neglecting inertia)

$$\Delta \mathbf{r} = \frac{6D\Delta t}{f\, b^2} \sum_{i=1}^{f} \frac{\mathbf{a}_i}{n_i} + \sqrt{\frac{12D\Delta t}{f}}\ \mathbf{u} \tag{2}$$

where **r** is node position, $D = kT/\zeta$ is subchain diffusivity (with the friction coefficient ζ taken as a constant), f is node functionality, **u** is a unit vector of random direction, and Δt is the time step. The first term in eq. (2) arises from the subchains pulling on the node, and the second from the stochastic force. The direction of the latter is random (as it should), and we have adopted, for simplicity, a fixed amplitude, taken in accordance with the fluctuation-dissipation theorem [14, 19]. In eq. (2), we have assumed that the node friction is $\zeta f/2$.

The other equation of motion describes chain sliding through sliplinks. Sliding of monomers results from a different tension in the two subchains belonging to the same chain (entering and leaving the sliplink), as well as from a stochastic force. The sliding equation is derived from the one-dimensional motion of a virtual bead located at the entanglement position (s=0). This virtual bead is pulled to one side or the other ($\Delta s > 0$ or < 0), resulting in an exchange of monomers Δn. The friction coefficient in the sliding motion is taken to be that of a subchain, i.e., ζ. The discretised equations (again for the Gaussian case) then read

$$\begin{aligned}
\Delta s &= \frac{3D\Delta t}{b^2}\left(\frac{a_j}{n_j} - \frac{a_i}{n_i}\right) \pm \sqrt{2D\Delta t} \\
\Delta n_i &= -n_i \frac{\Delta s}{\Delta s + a_i} \qquad \text{if } \Delta s > 0 \\
\Delta n_j &= -n_j \frac{-\Delta s}{-\Delta s + a_j} \quad \text{if } \Delta s < 0 \\
\Delta n_i &+ \Delta n_j = 0
\end{aligned} \tag{3}$$

where i and j indicate consecutive subchains along the same chain, and the one-dimensional random force is accounted for through the ± term. To guarantee that n never becomes negative, the change in n, Δn, is always calculated first for the subchain which looses monomers, with a formula (controlled by the sign of Δs) that automatically guarantees $|\Delta n| < n$. In particular, the formula is written by assuming constant monomer density along that subchain. The last of eqs. (3) assures that the total number of monomers in the two subchains is conserved.

Equilibration of the network is achieved by randomly picking a node and moving it according to eq. (2). If the node is a sliplink, eq. (3) is used first, once for each chain forming the entanglement. During this operation all other beads are kept fixed. Time is incremented by Δt after

all nodes have been moved once (on average). Approach to equilibrium is monitored through the total energy of the entropic springs. A constant energy (to within fluctuations) is considered a trustworthy indication of equilibrium. We have checked that also other quantities remain constant, such as the average distance between consecutive beads, etc. Results are calculated by averaging at three consecutive levels: (i) A first average is taken over all subchains at a given time for a given network realisation. (ii) That value is then averaged over time (under equilibrium conditions) to smooth out fluctuations. (iii) Since each network realisation has a quenched topology, a general average over many realisations is finally calculated. Following a standard procedure (*e.g.*, see [19]), determination of any average quantity was in fact repeated for several Δt values, and the extrapolation to $\Delta t=0$ was made.

A deformed state is achieved by first moving the box boundaries and all beads in the box (plus their periodic images) affinely, and subsequently letting the network relax. After relaxation the network behaves as if the deformation were imposed at infinity. The resulting stress tensor **T** is calculated as [14]

$$\mathbf{T} = \nu \left\langle \mathbf{F}\,\mathbf{a} \right\rangle \tag{4}$$

where ν is the subchain density. In this paper, we will only consider the stress difference $T_{xx} - T_{yy}$ generated by a volume preserving elongation of stretch-ratio λ in the x-direction.

Results and discussion

Typical simulation results are reported in the Mooney plots of Fig. 1, both for Gaussian and for finitely extensible chains, and compared with the theoretical predictions by Ball et al. [8] and Edwards and Vilgis [10], respectively. We recall that the theory of Ball et al. [8] contains a "sliding parameter" η, set by the authors themselves at the value $\eta = 0.234$. Such a value was derived by assuming that each sliplink can only slide up to the next one along the chain, in each of the two possible directions. In the theory of Edwards and Vilgis [10], together with η, a finite-extensibility parameter also appears, namely $\alpha = \langle n \rangle^{-1/2}$, where $\langle n \rangle$ is the mean number of monomers per subchain (50 in Fig. 1)

Figure 1a refers to the Gaussian case, with a number of entanglements per chain N=8. The symbols are simulation results, and the curve is the theory of Ball et al. [8] with $\eta = 0.234$. The modulus at small deformations obtained from our simulation coincides with the theoretical value.

Conversely, for larger deformations, the simulation generates a higher modulus than predicted by theory. We will comment on this discrepancy later in this section.

Figure 1b refers to the non-Gaussian case, and the curves are now from the theory of Edwards and Vilgis [10]. The full line is obtained by setting $N = 8$ and $\eta = 0.234$ (as in the Gaussian case), and $\alpha = 50^{-1/2} = 0.14$, consistently with the <n> value of our simulations. In comparing our results (filled circles) with the theoretical prediction, we find again that, at very small deformations, simulation and theory essentially coincide. We note in particular that the increase of modulus due to finite extensibility, predicted by Edwards and Vilgis [10], is quantitatively reproduced by the simulation. At larger deformations the quantitative situation deteriorates, however. As for the Gaussian case, our modulus falls off less steeply than predicted by theory. On the other hand, the upturn (which reveals closeness to full extension of the subchains) is slightly postponed to higher deformations, so that simulation and theory cross one another.

Figure 1b also reports the simulation results (open circles) of Grest et al. [13] for $N = 4$ (the largest N value run by them) and $<n> = 72$, to be compared with the corresponding prediction (dashed line) by Edwards and Vilgis ($N = 4$, $\alpha = 72^{-1/2} = 0.12$). The results by Grest et al. [13] run lower than the theoretical curve over the whole deformation range, though the slope is comparable.

The major difference between our coarse-grained simulations and both theory [8, 10] and "atomistic" simulations [13] is that our modulus does not decrease enough with increasing deformation. Insofar as a decreasing modulus is related to sliding through entanglements, we have then investigated how large is the average sliding in our simulations as a function of deformation. Figure 2a reports the standard deviation σ_n of the function n(t) measuring the number of monomers which at time t (starting from an arbitrary origin) have slid through a sliplink according to eqs. (3). Of course, n(t) fluctuates between positive and negative values. Figure 2a gives the ratio $\sigma_n / <n>$ as a function of deformation for the Gaussian case with $N = 8$. These results clearly show that, in our simulation, the extent of the sliding through entanglements decreases with increasing deformation, whereas in theory the sliding parameter η is kept constant, implying a deformation-independent extent of monomer fluctuations through sliplinks.

To confirm this conclusion, we have forced in the Gaussian theory [8] a λ-dependent sliding parameter η, such that the theoretical predictions coincide with our results. From a given η value, the quantity called x by Ball et al. [8] (a nondimensional measure of the extent of sliding) is calculated by inverting their eq. (50). Figure 2b shows x thus obtained as a function of λ. Figure 2b confirms that the extent of sliding must significantly decrease with increasing λ, if we want that theory and simulations agree with each other. Figure 2b also shows that the theoretical value $x = 1$ (corresponding to $\eta = 0.234$) is only approached at small deformations.

Although Fig. 2 explains the observed discrepancy between a constant-η theory and our simulations, there remains to understand which of the two predictions is closer to reality. This can be achieved by comparing the slope in the Mooney plot of Fig. 1 both with data and with the more detailed simulations of Grest et al. [13]. Figure 1b already showed that the steeper slope predicted by theory is essentially confirmed by Grest et al. simulations, and a similar conclusion is reached when comparing theory with data (see *e.g.* [21]). We are forced to conclude that our simulation requires some modification.

At first sight, our simulation scheme does not seem easy to modify, since it appears to contain all the essential physics. We envisage, however, the possibility of changing the ratio of the 3D node diffusivity in eq. (2) to the 1D sliding diffusivity in eq. (3), which was assumed equal to ½ in this work. In this regard, notice that changing the magnitude of the diffusivities, while not changing their ratio, does not modify equilibrium results, but only the relaxation kinetics. Conversely, changing the diffusivity ratio certainly affects equilibrium results. It should be sufficient to consider that if the sliding diffusivity is reduced to zero, sliplinks are effectively converted into crosslinks, and the slope in the Mooney plot becomes zero. We would therefore expect that if, on the contrary, we increase the sliding diffusivity with respect to that of the nodes, the modulus slope might increase. However, we must leave this analysis to future work.

Before concluding, we wish to emphasise how well the model behaves at small deformations. Figure 3 shows the small-deformation modulus obtained from the stress-strain isotherms of several non-Gaussian simulations (with $\langle n \rangle = 50$) as a function of the fraction of crosslinks $\varphi_{CL}=1/(N+1)$. Figure 3 also reports the corresponding theoretical prediction of Edwards and Vilgis [10]. The simulation results in Fig. 3 could be easily fitted to a straight line (though not exactly coincident with the theoretical one), thus confirming the assumption made by theory that contributions from slip- and cross-links are additive.

Figure 3 also shows two values of moduli taken from the simulations of Grest et al. [13] for dry rubbers, for which they estimate that the monomer number in subchains (i.e., between consecutive entanglements) is $\langle n \rangle = 72$. In their Fig. 2, three simulation results are reported, one of which seemingly refers to an entanglement-free rubber (since the chain monomers are $35 \ll 72$), while for the other two (chain monomers = 100 and 350) chains are long enough to imply the existence of entanglements. From the modulus ratio of the latter two data points to the first, we have obtained the results reported in Fig. 3. Accounting for error bars, and for the difference between the $\langle n \rangle$-values in our and their simulations, it appears that at small deformations our results do not differ much from those of Grest et al. [13].

Conclusions

We have presented a new coarse-grained simulation model for polymer networks with entanglements. The results for monodisperse networks confirm that the free energies of crosslinks and sliplinks are additive, as often assumed in rubber theories. Qualitatively, simulations of uniaxial extension reproduce the C_2 term of the Mooney-Rivlin expression in the presence of entanglements, as well as the strain hardening at even larger deformations. As regards quantitative comparison with the theories of Ball *et al*. [8] and Edwards and Vilgis [10], our simulations agree with the predicted dependence of the low-deformation modulus on entanglement concentration. At large deformations, however, we obtain a higher modulus than predicted by theory [8, 10], by Kremer *et al*. atomistic simulations [11-13], and shown by data [21]. The source of the discrepancy is still unclear, though we suspect that one factor could be the diffusivity ratio between the 3D node motion and the 1D sliding of chains along their contour. A minor discrepancy with theory concerns the location of the upturn predicted for the non-Gaussian case. This can perhaps be attributed to sliding of monomers over entanglements, which is ignored in the non-Gaussian correction of the theory [10], while it is included in our simulation.

We wish to emphasise that, since polymer molecules are here coarse-grained at the level of subchains between network nodes (either entanglements or crosslinks), rheological results can be obtained without using supercomputers. Thus, once the simulation model is suitably amended to pass the test of large deformations, it will allow for an easy exploration of various non-monodisperse networks with arbitrary functionality. The simplicity of the simulation model presented here also allows for an extension to the case of entangled melts or solutions [15], for which many-chain simulations of highly entangled polymers had not been previously developed.

Acknowledgements: Work supported by the EU under contract number FMRX–CT98-0210.

References

[1] Treloar L. R. G., *The Physics of Rubber Elasticity* (Clarendon Press, Oxford) 1975.

[2] Sharaf M.A., Mark J.E. and Alshamsi A.S., *Polymer J.*, **28** (1996) 375.

[3] James H. M. and Guth E., *J. Chem. Phys.*, **15** (1947) 669.

[4] Flory P. J., *J. Chem. Phys.*, **66** (1977) 5720.

[5] Erman B. and Monnerie L., *Macromolecules*, **22** (1989) 3342.

[6] Edwards S.F., *Proc. Phys. Soc. (London)*, **92** (1967) 9.

[7] Edwards S. F. and Vilgis T. A., *Rep. Prog. Phys.*, **51** (1988) 243.

[8] Ball R. C., Doi M., Edwards S. F. and Warner M., *Polymer*, **22** (1981) 1010.

[9] Panyukov S. V., *Sov. Phys. JETP*, **67** (1988) 2274.

[10] Edwards S. F. and Vilgis T. A., *Polymer*, **27** (1986) 483.

[11] Duering E. R., Kremer K. and Grest G. S., *J. Chem. Phys.*, **101** (1994) 8169.

[12] Pütz M., Kremer K. and Everaers R., *Phys. Rev. Lett.*, **84** (2000) 298.

[13] Grest G. S., Pütz M., Everaers R. and Kremer K., *J. Non-Cryst. Solids*, **274** (2000) 139.

[14] Doi M. and Edwards S. F., *The Theory of Polymer Dynamics* (Clarendon Press, Oxford) 1986.

[15] Masubuchi Y., Takimoto J., Koyama K., Ianniruberto G., Greco F. and Marrucci G., *J. Chem. Phys.*, **115** (2001) 4387.

[16] Ben-Naim E., Grest G. S., Witten T. A. and Baljon A. R. C., *Phys. Rev. E*, **53** (1996) 1816.

[17] Boué F., Bastide J., Buzier M., Lapp A., Collette C. and Herz J., *Prog. Coll. Polymer Sci*., **75** (1987) 152.

[18] Warner H. R., *Ind. Eng. Chem. Fundam.*, **11** (1972) 379.

[19] Honerkamp J., *Stochastic Dynamical Systems* (VCH, New York) 1994.

[20] Fetters L. J., Lohse D. J., Richter D., Witten T. A., and Zirkel A., *Macromolecules*, **27** (1994) 4639.

[21] Rubinstein M. and Panyukov S. V., *Macromolecules*, **30** (1998) 8036.

Figure Captions

Figure 1: Mooney plot of stress-strain isotherms. (a) Gaussian chains; full curve is Ball *et al*. theory [8], and symbols are our simulations. (b) Non-Gaussian case; curves are from the theory of Edwards and Vilgis [10] for N=8, <n>=50 (full line), and for N=4, <n>=72 (dashed line); full circles are our simulations (to be compared with full line), empty circles are simulations of Grest et al. [13] (to be compared with dashed line).

Figure 2: Estimate of the extent of monomer sliding through sliplinks for Gaussian chains with N = 8. (a) Direct results from our simulations. (b) Indirect results in terms of the quantity x (related to η) in Ball et al. [8].

Figure 3: The shear modulus at small deformations *vs*. the cross-link fraction φ_{CL}. Simulation results (full symbols) were obtained by interpolating at zero strain (λ=1) the stress-strain isotherms for compression and extension of non-Gaussian chains with <n>=50. The straight line is the corresponding prediction from the theory of Edwards and Vilgis [10]. Empty symbols are molecular dynamics results (with <n>=72) taken from Fig. 2 in Grest et al [13], with an error bar of 10 % as indicated by them.

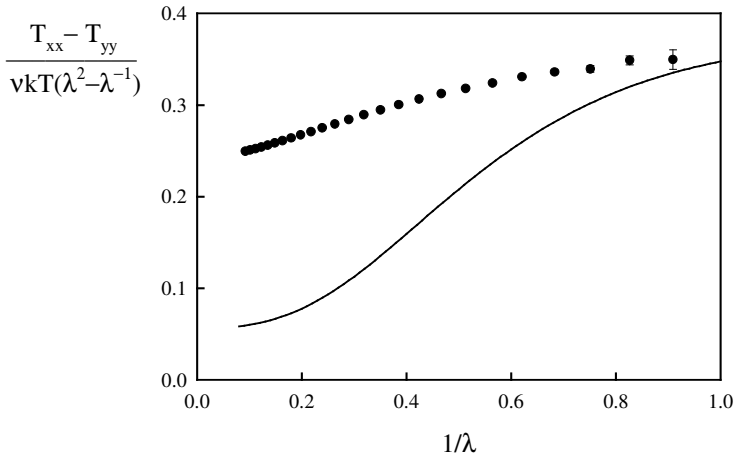

(1a)

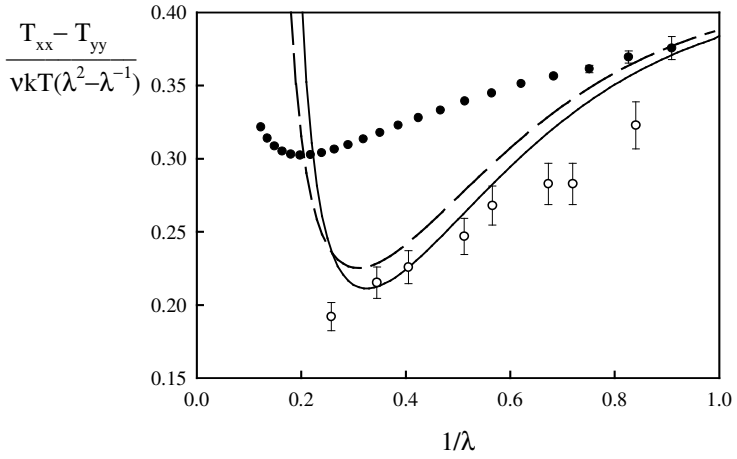

(1b)

Figure 1

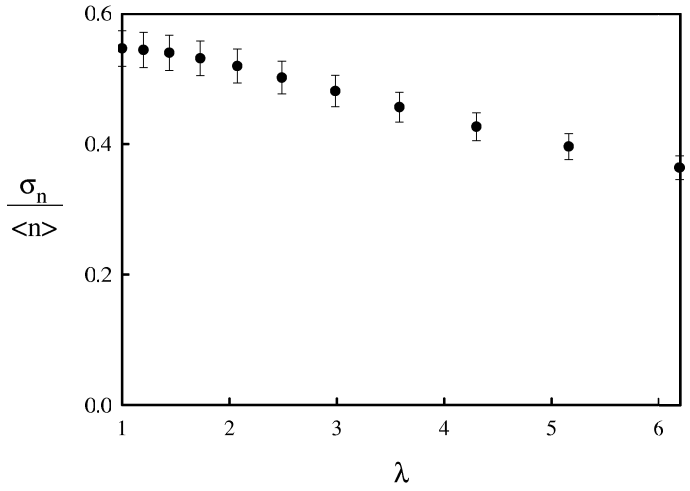

(a)

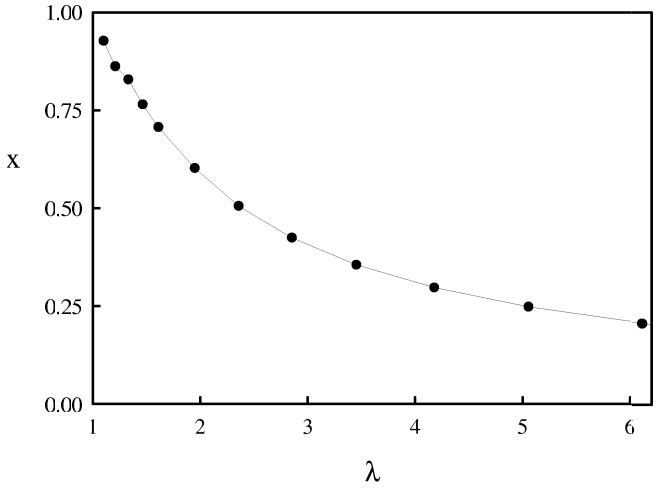

(b)

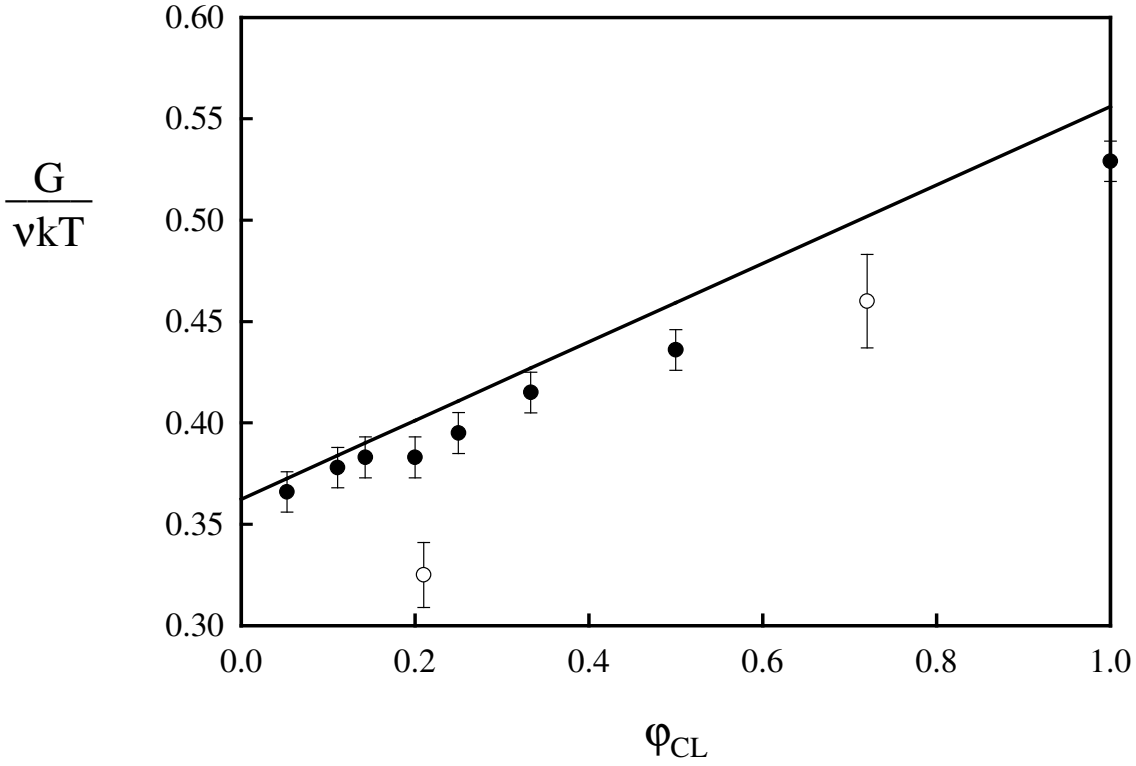

Figure 3